A Level-Increased Nearest Level Modulation Method for Modular Multilevel Converters

Pengfei Hu, *Student Member, IEEE*, and Daozhuo Jiang

***Abstract*—The modular multilevel converter (MMC) is emerging to be a promising approach for medium- and high-voltage applications. This paper proposes a modified nearest level modulation (NLM) method for the MMC, with which the level number of ac output voltage increases to $2N + 1$ (where N is the submodule numbers per arm) as great as that of the carrier-phase-shifted PWM and the improved submodule unified PWM methods. The level number is almost doubled and the height of the step in the step wave is halved. Therefore, the ac output voltage waveform quality using the proposed method is better than that using the conventional NLM method. Besides, the proposed method keeps the conventional NLM method's characteristics such as low switching frequency and simple implementation. The performance of the proposed method is verified by simulations and experiments using a laboratory-scale prototype.**

***Index Terms*—Modular multilevel converters (MMCs), nearest level modulation (NLM), prototype, 2N + 1 level.**

NOMENCLATURE

u	Ac output voltage
u_U	Upper-arm voltage
u_L	Lower-arm voltage
u_U^{ref}	Reference value of upper-arm voltage
u_L^{ref}	Reference value of lower-arm voltage
L	Arm inductor
i	Ac current
u_e	Ac electromotive force
u_e^{ref}	Reference value of ac electromotive force
U_{dc}	Dc voltage
m	Modulation ratio
ω	Angle frequency
N	Submodule number per arm
N_U	Submodule number in the upper arm
N_L	Submodule number in the lower arm
U_d	Rated voltage of submodule capacitor
u_U^{step}	Step wave of the upper-arm voltage
u_L^{step}	Step wave of the lower-arm voltage
u_e^{step}	Step wave of ac electromotive force

Manuscript received November 16, 2013; revised April 3, 2014; accepted March 31, 2014. Date of publication May 20, 2014; date of current version November 3, 2014. Recommended for publication by Associate Editor J. Clare.

The authors are with the College of Electrical Engineering, Zhejiang University, Hangzhou 310027, China (e-mail: eehpf@zju.edu.cn; dzjiang@zju.edu.cn).

Color versions of one or more of the figures in this paper are available online at http://ieeexplore.ieee.org.

Digital Object Identifier 10.1109/TPEL.2014.2325875

I. INTRODUCTION

THE modular multilevel converter (MMC) is being conjectured as the most promising multilevel power converter for medium- and high-voltage range applications such as high-voltage direct current (HVDC) transmissions [1]–[3], transformerless static synchronous compensators (STATCOMs) [4], [5], high-power motor drives [6]–[9], electric railway supplies [10], and unified power flow controllers (UPFCs) [11].

In recent years, the MMC has attracted much attention by academic scholars resulting in large numbers of research publications, which focus on mathematical modeling [12]–[14], modulation methods [15]–[18], control strategies [19]–[25], capacitor voltage balancing [26], simulation techniques [27], circulating current suppressing [28], [29], fault detection [30], and so on. As to the modulation methods for MMCs, there are mainly two types [i.e., pulse width modulations (PWMs) and step wave modulations]. Furthermore, PWM methods include the carrier-phase-shifted PWM (CPSPWM) [17], the submodule unified PWM (SUPWM) [31], and the improved SUPWM [16], sharing some common features such as high switching frequency, large switching losses, and complex implementation process. Among the PWM methods, the CPSPWM and improved SUPWM can generate output voltages with $2\ N\ +\ 1$ levels, while the conventional SUPWM can only generate output voltages with $N + 1$ levels. As for step wave modulation methods, they mainly include selective harmonic elimination (SHE) method [14] and nearest level modulation (NLM) method [32], which share some common characteristics such as low switching frequency and N+1 levels. Compared to the SHE method, the NLM method does not need a complex calculation of the trigger angles, making NLM method the simplest and most practical modulation method for the MMC. However, in spite of the low switching frequency and simple implementation, the NLM method generates poorer quality waveforms than the CPSPWM and the improved SUPWM methods in case of small numbers of sub-modules. Therefore, the NLM method is mainly applied in high voltage applications where the step number is large enough to improve the output voltage. In order to improve the performance of the NLM method in case of a small number of submodules, this paper proposes a modified NLM method with which the maximum level number reaches $2N + 1$ as the same as that with the CPSPWM and the improved SUPWM methods.

The outline of this paper is organized as follows: principles of the MMC are briefly presented in Section II. In Section III, the conventional NLM method is introduced. In Section IV, a modified NLM method is proposed and analyzed.

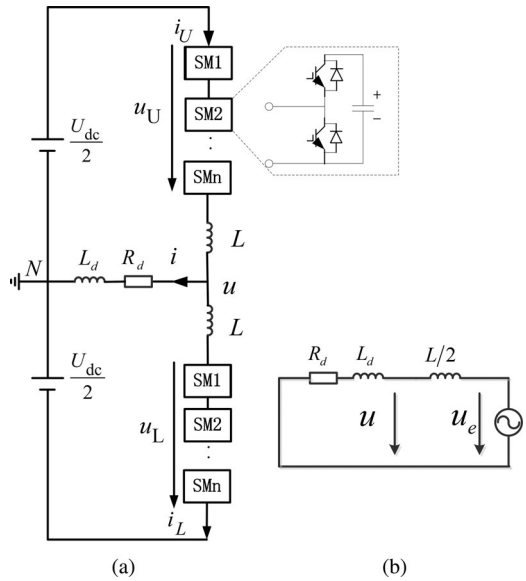

Fig. 1. (a) Topology of the single-phase MMC; (b) equivalent circuit of the MMC.

In Section V, simulation and experimental results validate the proposed method.

II. Principles of the MMC

The topology of a single-phase MMC as shown in Fig. 1(a) consists of the upper and lower arms, each formed by N series-connected identical half-bridge submodules as well as one arm inductor. Applying Kirchhoff's voltage law and Kirchhoff's current law in Fig. 1(a) yields

$$\begin{cases} u = -u_U - L\dfrac{di_U}{dt} + \dfrac{1}{2}U_{\rm dc} \\ u = u_L + L\dfrac{di_L}{dt} - \dfrac{1}{2}U_{\rm dc} \end{cases} \tag{1}$$

$$i = i_L - i_U. \tag{2}$$

The equivalent circuit of the MMC is shown in Fig. 1(b). From (1) and (2), the output voltage can be expressed as

$$u = \frac{1}{2}(u_L - u_U) + \frac{L}{2}\frac{di}{dt}. \tag{3}$$

It can be seen from (3) that the ac electromotive force (EMF) of the MMC is written as

$$u_e = \frac{1}{2}(u_L - u_U). \tag{4}$$

In general, the reference value of ac EMF is expressed as

$$u_e^{\rm ref} = \frac{mU_{\rm dc}}{2}\cos(\omega t) \tag{5}$$

where m($0 \le m \le 1$) is the modulation index and is the angular frequency. With the conventional NLM method, *N* submodules are inserted in the circuit. Therefore, the following equation is satisfied on the dc side.

$$U_{\rm dc} = u_U + u_L. \tag{6}$$

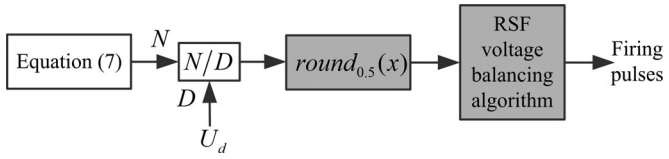

Fig. 2. Overall diagram of the conventional NLM method.

From (5) to (7), reference voltages of the upper and lower arms are determined by

$$\begin{cases} u_U^{\rm ref} = \frac{U_{\rm dc}}{2}[1 - m\cos(\omega t)] \\ u_L^{\rm ref} = \frac{U_{\rm dc}}{2}[1 + m\cos(\omega t)] \end{cases}. \tag{7}$$

Without redundant submodules, the submodule capacitor voltage and the dc voltage satisfy the following equation:

$$U_{\rm dc} = NU_d. \tag{8}$$

III. Conventional NLM Method

Fig. 2 shows the overall diagram of the conventional NLM method using the reduced switching-frequency voltage balancing algorithm [28]. The inserted submodule numbers of the upper and lower arms are calculated by

$$\begin{cases} N_U = {\rm round}_{0.5}\left\{\frac{U_{\rm dc}}{2U_d}[1 - m\cos(\omega t)]\right\} \\ N_L = {\rm round}_{0.5}\left\{\frac{U_{\rm dc}}{2U_d}[1 + m\cos(\omega t)]\right\} \end{cases}. \tag{9}$$

The round function (${\rm round}_{0.5}(x)$) means that the real number *x* is rounded to the nearest whole number according to the decimal fraction of *x*. If the decimal fraction of *x* is bigger than 0.5, *x* is rounded up to the next whole number, otherwise rounded down to the next whole number.

Fig. 3 illustrates the operation principles of both the conventional and modified NLM methods using an MMC with ten submodules per arm. To understand the principle of the conventional NLM method, two cases [t_1 to t_2, t_2 to t_3 in Fig. 2(a)] are analyzed. Assuming $u_L^{\rm step} = MU_d$ in the first case (i.e., from t_1 to t_2), reference values of arm voltages and ac EMF at $t = t_1$ can be expressed as

$$\begin{cases} u_L^{\rm ref} = (M + 0.5)U_d \\ u_U^{\rm ref} = [(N - M - 1) + 0.5]U_d \end{cases} \tag{10}$$

$$u_e^{\rm ref} = (M - 0.5N + 0.5)U_d. \tag{11}$$

In the first case, the step waves of arm voltages and ac EMF are expressed as

$$\begin{cases} u_L^{\rm step} = MU_d \\ u_U^{\rm step} = (N - M)U_d \end{cases} \tag{12}$$

$$u_e^{\rm step} = (M - 0.5N)U_d. \tag{13}$$

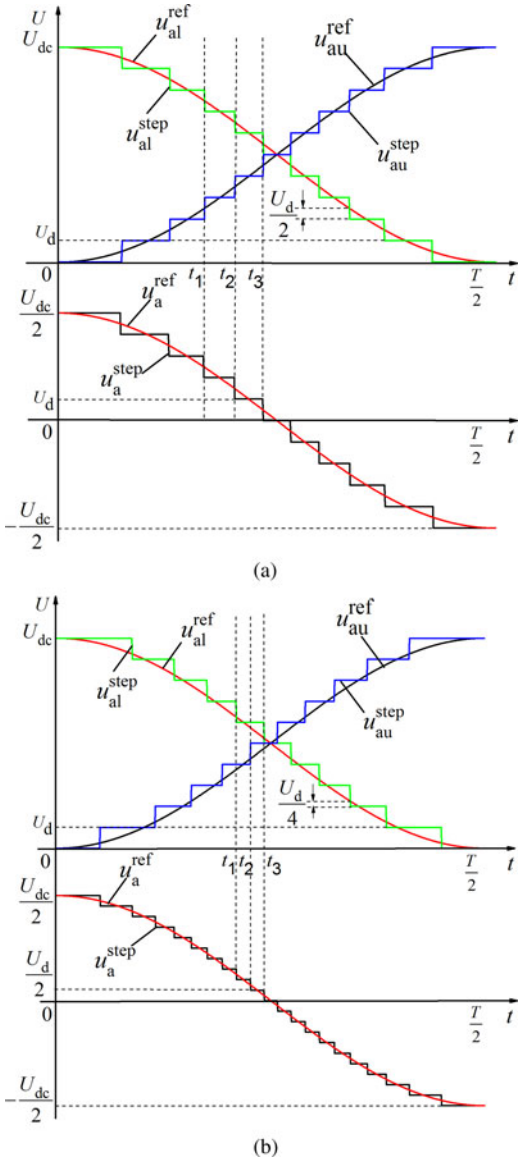

Fig. 3. (a) Principles of the conventional NLM method. (b) Principles of the modified NLM method.

The second case is from t_2 to t_3. Reference values of arm voltages and ac EMF at $\mathrm{t} = t_2$ can be expressed as

$$\begin{cases} u_L^{\mathrm{ref}} = [(M-1)+0.5]U_d \\ u_U^{\mathrm{ref}} = [(N-M)+0.5]U_d \end{cases} \tag{14}$$

$$u_e^{\mathrm{ref}} = (M-0.5N-0.5)U_d. \tag{15}$$

In the second case, the step waves of arm voltages and ac EMF are expressed as

$$\begin{cases} u_L^{\mathrm{step}} = (M-1)U_d \\ u_U^{\mathrm{step}} = (N-M+1)U_d \end{cases} \tag{16}$$

$$u_e^{\mathrm{step}} = (M-0.5N-1)U_d. \tag{17}$$

Comparing (13) and (17), it can be seen that the step height in u_e^{step} is U_d. Because the positive and negative dc voltage limits

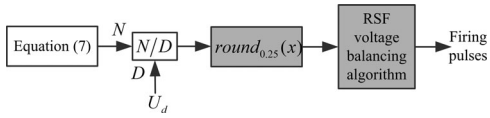

Fig. 4. Overall diagram of the modified NLM method.

are $\pm 0.5U_{\mathrm{dc}}$, the maximum level number in ac EMF is equal to $U_{\mathrm{dc}}/U_d + 1$ (i.e., $N+1$). The maximum error between u_e^{ref} and u_e^{step} appears at the moment of step changing (i.e., t_1, t_2, and t_3). Comparing (11) and (13) or (15) and (17), it is obvious that the maximum error is $0.5U_d$.

IV. Modified NLM Method

As analyzed previously, the conventional NLM method generates $N+1$ level waveform. Therefore, in the low-voltage situation with a few submodules, the total harmonic distortion (THD) of the output voltage tends to be large. To improve the output voltage quality, a modified NLM method is proposed in this section. With the proposed method, the number of the output level increases to as great as $2N+1$ under the condition of the same number of submodules.

Fig. 3(b) illustrates the principle of the modified NLM method. It is worth noting that the moments of step changing in u_L^{step} and u_U^{step} are not exactly the same. The level numbers of arm voltages are $N+1$, while the level number of output voltage is $2N+1$. Moreover, the step height of the output voltage is decreases to $0.5U_d$. This little difference leads to substantially increased levels.

To shift the moments of step changing in the upper- and lower-arm voltages, the arm inserted submodule numbers should be modified as expressed in (18)

$$\begin{cases} N_U = \mathrm{round}_{0.25}\left\{\dfrac{U_{\mathrm{dc}}}{2U_d}[1-m\cos(\omega t)]\right\} \\ N_L = \mathrm{round}_{0.25}\left\{\dfrac{U_{\mathrm{dc}}}{2U_d}[1+m\cos(\omega t)]\right\} \end{cases}. \tag{18}$$

The round function ($\mathrm{round}_{0.25}(x)$) means that the real number x is rounded to the nearest whole number according to the decimal fraction of x. If the decimal fraction of x is bigger than 0.25, x is rounded up to the next whole number, otherwise rounded down to the next whole number. The overall diagram of the modified NLM method is illustrated in Fig. 4.

A. Principles of the 2N + 1 Level

The difference between the proposed method and the conventional method is the round function. Two cases of the proposed method are illustrated in Fig. 3(b).

The first case is from t_1 to t_2. Assuming $u_L^{\mathrm{step}} = MU_d$ in the first case, reference values of arm voltages and ac EMF at $t = t_1$ can be expressed as

$$\begin{cases} u_L^{\mathrm{ref}} = (M+0.25)U_d \\ u_U^{\mathrm{ref}} = [(N-M-1)+0.75]U_d \end{cases} \tag{19}$$

$$u_e^{\mathrm{ref}} = (M-0.5N+0.25)U_d. \tag{20}$$

According to the modified round function, the step waves of arm voltages and ac EMF in the first case are expressed as

$$\begin{cases} u_L^{\text{step}} = MU_d \\ u_U^{\text{step}} = (N-M)U_d \end{cases} \tag{21}$$

$$u_e^{\text{step}} = (M - 0.5N)U_d. \tag{22}$$

The second case is from t_2 to t_3, reference values of arm voltages and ac EMF at $t = t_2$can be expressed as

$$\begin{cases} u_L^{\text{ref}} = [(M-1) + 0.75]U_d \\ u_U^{\text{ref}} = [(N-M) + 0.25]U_d \end{cases} \tag{23}$$

$$u_e^{\text{ref}} = (M - 0.5N - 0.25)U_d. \tag{24}$$

The step waves of arm voltages and ac EMF in the second case are expressed as

$$\begin{cases} u_L^{\text{step}} = MU_d \\ u_U^{\text{step}} = (N-M+1)U_d \end{cases} \tag{25}$$

$$u_e^{\text{step}} = (M - 0.5N - 0.5)U_d. \tag{26}$$

Comparing (22) and (26), it can be seen that the height of step in u_e^{step} is $0.5U_d$. Because the positive and negative dc voltage limits are $\pm 0.5U_{\text{dc}}$, the maximum level number in ac EMF is equal to $U_{\text{dc}}/0.5U_d + 1$ (i.e., $2N + 1$). The maximum error between u_e^{ref} and u_e^{step} appears at the moments of step changing (i.e., t_1, t_2 and t_3). Comparing (19) and (20) or (24) and (26), it is obvious that the maximum error is $0.25U_d$. Compared to the conventional method, the proposed method almost doubles the output level number. It leads to considerable suppression of the ac output harmonics and EMI noise caused by dv/dt.

Compared to the conventional method, the proposed method almost doubles the output level number. It leads to considerable suppression of the ac output harmonics and EMI noise caused by dv/dt. Also, the proposed method has low switching frequency than the improved SUPWM method presented in [16].

B. Voltages on the dc Side

With the conventional NLM method, it is worth noting in (12) and (16) that the sum of u_L^{step} and u_U^{step} is always NU_d. In other words, the total number of the inserted submodules is a constant N. However, with the modified NLM method the sum of u_L^{step} and u_U^{step} is, respectively, in (21) and in (25). The total number of the inserted submodules varies between N and $N+1$. This change makes pulse voltages appear across the arm inductors.

V. Simulation and Experimental Results

In order to verify the proposed method in both the grid-connected and load-connected situations, a three-phase MMC simulation model and a single-phase MMC prototype are presented.

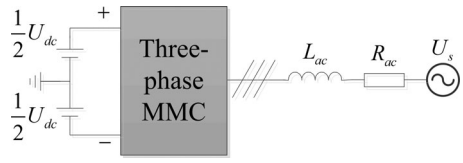

Fig. 5. Setup of the three-phase MMC for simulation.

TABLE I
Main Circuit Parameters for Simulations

Items	Symbols	Values
Rated ac line-line voltage	U_s	35 kV
ac system inductance	L_{ac}	5 mH
ac system resistance	R_{ac}	0.03 ohm
Rated frequency	f	50 Hz
Rated direct voltage	U_{dc}	±5 kV
Arm inductance	L	15 mH
Total number of SMs per arm	N	10
Capacitor voltage	U_d	1 kV
SM capacitance	C	7000 uF

A. Simulation Results

The setup of the three-phase MMC for simulation is shown in Fig. 5. The simulation is carried out in the PSCAD/EMTDC software with circuit parameters listed in Table I.

To demonstrate the effectiveness of the modified NLM method, a comparison between the conventional NLM method and the modified NLM method is made in the simulation. Initially, the conventional NLM method is adopted in the MMC. The active current reference (i_d^{ref}) is set to 0.2 kA (let the direction from the grid to the MMC positive). At $t = 0.5$ s, the modified NLM method is enabled with the same power transmission.

Figs. 6–8 show the simulation results with both the conventional and modified NLM methods. When using the conventional NLM method, the three-phase ac voltages on the converter side appear evident distortion and the THD reaches 5.90%. Since currents flow through the submodule capacitors, the steps are smoothed by the fluctuation of submodule capacitor voltages. Anyway, it also can be seen 11 levels in the ac voltages. Besides, the THD of three-phase ac currents reaches 4.86%, which is caused by the harmonics of the ac voltages.

When using the modified NLM method, THDs of the three-phase ac voltages and currents are reduced to 2.02% and 0.79%, respectively. The voltage steps are too many and small to recognize. Moreover, the submodule capacitor voltages decrease a little with the modified NLM method as shown in Fig. 7. This is because the total number of inserted submodules varies between N and $N+1$ (i.e., equivalent number is greater than N) with the modified NLM method. The variation of the total number of inserted submodule also leads to larger voltage across the upper and lower arm inductors as shown in Fig. 7. Fig. 8 shows that the error in i_d is reduced with the modified NLM method.

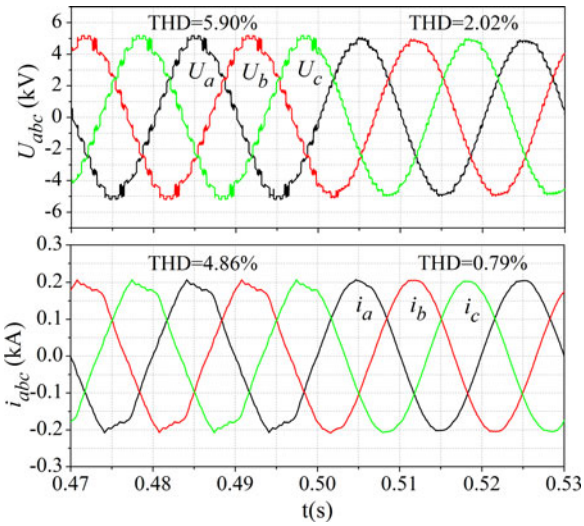

Fig. 6. Three-phase ac voltages and currents.

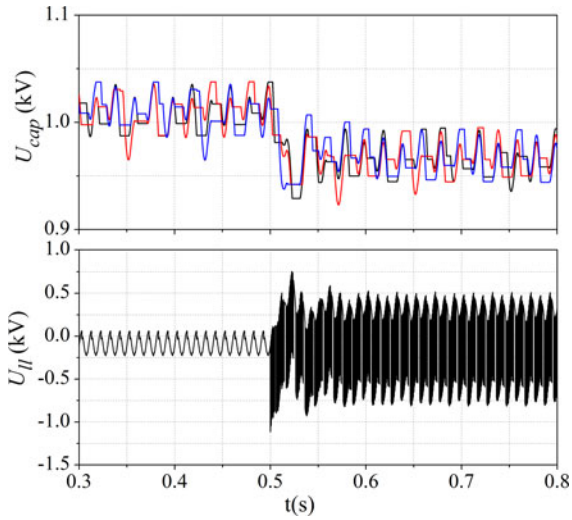

Fig. 7. Capacitor voltages of submodules ($U_{\rm cap}$) and the voltage across the upper and lower inductors (U_{ll}).

B. Experimental Results

The circuit topology of the single-phase MMC prototype is illustrated in Fig. 1 and the photo of the prototype is shown in Fig. 9. To validate the proposed method, experiments are carried out on the prototype with circuit parameters listed in Table II. The main circuit uses MOSFET as the power switch. The control system includes two-level structure implemented by FPGA and NI CompactRIO. Optical fibers are used to transmit necessary signals (i.e., trigger pulses, submodule capacitor voltages, and protective signals) between the main circuit and control system. The dc voltage is supplied by a three-phase diode rectifier connected to a voltage regulator.

Figs. 10 and 11 show the experimental results with the conventional NLM method and the modified NLM method, respectively. Because the modulation ratio is 0.9, it is easily seen that the ac output voltage (u) includes nine levels in Fig. 10 and 17 levels in Fig. 9. Due to the limitation of experimental conditions, only the upper arm current is measured. As shown in Fig. 10, the voltage across the arm inductors (u_{ll}) tends to be zero regardless of the voltage spikes caused by the dead-time effect. On the contrary, u_{ll} in the Fig. 11 tends to be larger. The switching frequency of the MOSFET with the conventional NLM method stands almost 300 Hz similar to the modified NLM method illustrated in $u_{\rm SM}$.

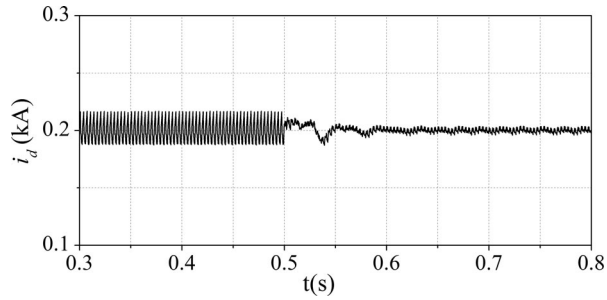

Fig. 8. Active current (i_d).

Fig. 9. Photo of the single-phase MMC prototype.

TABLE II
MAIN CIRCUIT PARAMETERS FOR EXPERIMENTS

Items	Symbols	Values
Rated frequency	f	50 Hz
Rated direct voltage	$U_{\rm dc}$	100 V
Modulation ratio	m	0.9
Arm inductance	L	15 mH
Total number of SMs per arm	N	10
Rated capacitor voltage	U_d	10 V
Capacitor capacitance	C	4000 uF
Load resistance	R_d	100 ohm
Load inductor	L_d	70 mH

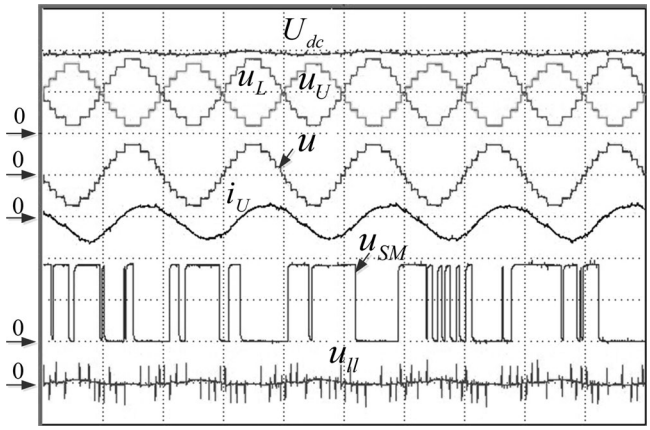

Fig. 10. Waveforms of experiment with the conventional NLM method: Direct voltage ($U_{\rm dc}$), vertical 50 V/div; arm voltages (u_U, u_L), vertical 50 V/div; ac output voltage (u), vertical 50 V/div; upper-arm current (i_U), vertical 0.5 A/div; output voltage of a sub-module ($u_{\rm SM}$), vertical 5 V/div; the voltage across the two inductors (u_{ll}), vertical 20 V/div; horizon 0.5 ms/div.

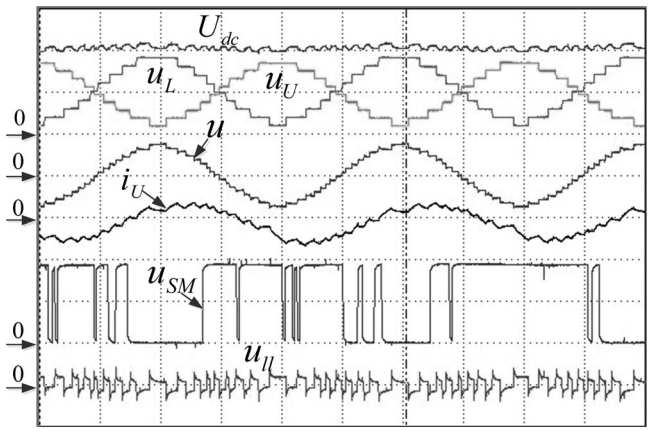

Fig. 11. Waveforms of experiment with the modified NLM method: Direct voltage ($U_{\rm dc}$), vertical 50 V/div; arm voltages (u_U, u_L), vertical 50 V/div; ac output voltage (u), vertical 50 V/div; upper-arm current (i_U), vertical 0.5 A/div; output voltage of a submodule ($u_{\rm SM}$), vertical 5 V/div; the voltage across the two inductors (u_{ll}), vertical 20 V/div; horizon 0.5 ms/div.

VI. Conclusions

A modified NLM method for modular multilevel converters, which can generate $2N + 1$ level ac output voltage, is proposed in this paper. The level number of ac output voltage with the modified NLM method is almost double than that with the conventional NLM method. Compared to the improved SUPWM and CPSPWM methods, which can both generate $2N + 1$ level ac output voltage, the modified NLM method has lower switching frequency. Principles of the modified NLM method are presented. Both simulation and experimental results validate the effectiveness of the modified NLM method.

References

[1] S. Allebrod, R. Hamerski, and R. Marquardt, "New transformerless, scalable modular multilevel converters for HVDC-transmission," in *Proc. IEEE Power Electron. Spec. Conf.*, 2008, pp. 174–179.

[2] Q. Jiangchao and M. Saeedifard, "Predictive control of a modular multilevel converter for a back-to-back HVDC system," *IEEE Trans. Power Del.*, vol. 27, no. 3, pp. 1538–1547, Jul. 2012.

[3] M. Guan and Z. Xu, "Modeling and control of a modular multilevel converter-based HVDC system under unbalanced grid conditions," *IEEE Trans. Power Electron.*, vol. 27, no. 12, pp. 4858–4867, Dec. 2012

[4] G. P. Adam, O. Anaya-Lara, G. Burt, and J. McDonald, "Transformerless STATCOM based on a five-level modular multilevel converter," in *Proc. 13th Eur. Conf. Power Electron. Appl.*, 2009, pp. 1–10.

[5] M. Hagiwara, R. Maeda, and H. Akagi. "Negative-sequence reactive-power control by a PWM STATCOM based on a modular multilevel cascade converter (MMCC–SDBC)," in *Proc. IEEE. Energy Convers. Congr. Expo.*, 2011, pp. 3728–3735.

[6] A. Antonopoulos, K. Ilves, L. Ängquist, and H.-P. Nee, "On interaction between internal converter dynamics and current control of high-performance high-power AC motor drives with modular multilevel converters," in *Proc. IEEE. Energy Convers. Congr. Expo.*, 2010, pp. 4293–4298.

[7] M. Hagiwara, K Nishimura, and H. Akagi, "A medium-voltage motor drive with a modular multilevel PWM inverter," *IEEE Trans. Power Electron.*, vol. 25, no. 7, pp. 1786–1799, Jul. 2010.

[8] A. J. Korn, M. Winkelnkemper, and P. Steimer, "Low output frequency operation of the modular multi-level converter," in *Proc. IEEE Energy Convers. Congr. Expo.*, 2010, pp. 3993–3997.

[9] A. Antonopoulos, L. Angquist, S. Norrga, K. Ilves, L. Harnefors, and H. Nee, "Modular multilevel converter ac motor drives with constant torque from zero to nominal speed," in *Proc. IEEE Energy Convers. Congr. Expo.*, 2012, pp. 749–746.

[10] M. Glinka and R. Marquardt, "A new AC/AC multilevel converter family," *IEEE Trans. Ind. Electron.*, vol. 52, no. 3, pp. 662–669, Jun. 2005.

[11] Z. Guying, J. Daozhuo, and L. Xiaorang, "Modular multilevel converter for unified power flow controller application," in *Proc. 3rd Int. Conf. Digital Manuf. Autom*, Jul. 31–Aug. 2, 2012., pp. 545–549.

[12] L. Harnefors, A. Antonopoulos, S. Norrga, L. Angquist, and H.-P. Nee, "Dynamic analysis of modular multilevel converters," *IEEE Trans. Ind. Electron.*, vol. 60, no. 7, pp. 2526–2537, Jul. 2013.

[13] A. Antonopoulos, L. Angquist, L. Harnefors, K. Ilves, and H.-P. Nee, "Global asymptotic stability of modular multilevel converters," *IEEE Trans. Ind. Electron.*, vol. 61, no. 2, pp. 603–612, Feb. 2014.

[14] D. C. Ludois, G. Venkataramanan, "Simplified terminal behavioral model for a modular multilevel converter," *IEEE Trans. Power Electron.*, vol. 29, no. 4, pp. 1622–1631, Apr. 2014.

[15] K. Ilves, A. Antonopoulos, S. Norrga, and H-.P. Nee, "A new modulation method for the modular multilevel converter allowing fundamental switching frequency," *IEEE Trans. Power Electron.*, vol. 27, no. 8, pp. 3482–3494, Aug. 2012.

[16] Z. Li, P. Wang, H. Zhu, Z. Chu, and Y. Li, "An improved pulse width modulation method for chopper-cell-based modular multilevel converters," *IEEE Trans. Power Electron.*, vol. 27, no. 8, pp. 3472–3481, Aug. 2012.

[17] M. Hagiwara and H. Akagi, "Control and experiment of pulsewidth-modulated modular multilevel converters," *IEEE Trans. Power Electron.*, vol. 24, no. 7, pp. 1737–1746, Jul. 2009.

[18] E. Solas, G. Abad, J. A. Barrena, A. Carcar, and S. Aurtenetxea, "Modulation of modular multilevel converter for HVDC application," in *Proc. 14th Int. Power Electron. Motion Control Conf.*, 2010, pp. T2-84–T2-89.

[19] Q. Jiangchao and M. Saeedifard, "Predictive control of a modular multilevel converter for a back-to-back HVDC system," *IEEE Trans. Power Del.*, vol. 27, no. 3, pp. 1538–1547, Jul. 2012.

[20] M. Guan and Z. Xu, "Modeling and control of a modular multilevel converter-based HVDC system under unbalanced grid conditions," *IEEE Trans. Power Electron.*, vol. 27, no. 12, pp. 4858–4867, Dec. 2012.

[21] M. Hagiwara, R Maeda, and H. Akagi, "Negative-sequence reactive-power control by a PWM STATCOM based on a modular multilevel cascade converter (MMCC–SDBC)," in *Proc. IEEE Energy Convers. Congr. Expo.*, 2011, pp. 3728–3735.

[22] L. Angquist, A. Antonopoulos, D. Siemaszko, K. Ilves, M. Vasiladiotis, and H.-P. Nee, "Open-loop control of modular multilevel converters using estimation of stored energy," *IEEE Trans. Ind. Appl.*, vol. 47, no. 6 pp. 2516–2524, Nov./Dec. 2011.

[23] T. S. Gum, H.-J. Lee, T. S. Nam, Y.-H. Chung, U.-H. Lee, S.-T. Baek, K. Hur, and J.-W. Park, "Design and control of a modular multilevel HVDC converter with redundant power modules for noninterruptible energy transfer," *IEEE Trans. Power Del.*, vol. 27, no. 3 pp. 1611–1619, Jul. 2012.

[24] Y. Zhou, D. Jiang, P. Hu, J. Guo, Y. Liang, and Z. Lin, "A prototype of modular multilevel converters," *IEEE Trans. Power Electron.*, vol. 29, no. 7, pp. 3267–3278, Jul. 2014.
[25] Y. Zhou, D. Jiang, J. Guo, P. Hu, and Y. Liang, "Analysis and control of modular multilevel converters under unbalanced conditions," *IEEE Trans. Power Del.*, vol. 28, no. 4, pp. 1986–1995, Oct. 2013.
[26] K. Wang, Y. Li, Z. Zheng, and L. Xu, "Voltage balancing and fluctuation-suppression methods of floating capacitors in a new modular multilevel converter," *IEEE Trans. Ind. Electron.*, vol. 60, no. 5, pp. 1943–1954, May 2013.
[27] U. N. Gnanarathna, A. M. Gole, and R. P. Jayasinghe, "Efficient modeling of modular multilevel HVDC converters (MMC) on electromagnetic transient simulation programs," *IEEE Trans. Power Del.*, vol. 26, no. 1, pp. 316–324, Jan. 2011.
[28] T. Qingrui, X. Zheng, and X. Lie, "Reduced switching-frequency modulation and circulating current suppression for modular multilevel converters," *IEEE Trans. Power Del.*, vol. 26, no. 3, pp. 2009–2017, Jul. 2011.
[29] K. Ilves, A. Antonopoulos, L. Harnefors, S. Norrga, and H.-P. Nee, "Circulating current control in modular multilevel converters with fundamental switching frequency," in *Proc. 7th Int. Power Electron. Motion Control Conf.*, Jun. 2–5, 2012, vol. 1, pp. 249–256.
[30] S. Shao, P. W. Wheeler, J. C. Clare, and A. J. Watson, "Fault detection for modular multilevel converters based on sliding mode observer," *IEEE Trans. Power Electron.*, vol. 28, no. 11, pp. 4867–4872, Nov. 2013.
[31] S. Rohner, S. Bernet, M. Hiller, and R. Sommer, "Modulation, losses, and semiconductor requirements of modular multilevel converters," *IEEE Trans. Ind. Electron.*, vol. 57, no. 8, pp. 2633–2642, Aug. 2010.
[32] M. Guan, Z. Xu, and H. Chen, "Control and modulation strategies for modular multilevel converter based HVDC system," in *Proc. 37th Annu. Conf. IEEE Ind. Electron. Soc*, Nov. 7–10, 2011, pp. 849–854.

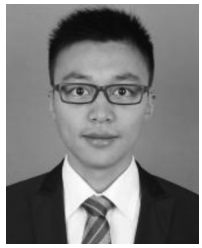

Pengfei Hu (S'13) was born in Suining, China, on January 8, 1988. He received the B.E. degree in electrical engineering and its automation from the College of Electrical Engineering, Zhejiang University, Hangzhou, China, in 2010, where he is currently working toward the Ph.D. degree.

His research interests include high voltage dc transmission and flexible ac transmission systems.

Daozhuo Jiang was born in Minhou, China, on July 21, 1960. He received the Graduation degree from the Department of Electrical Engineering, Zhejiang University, Hangzhou, China.

He is currently a Professor with the College of Electrical Engineering, Zhejiang University. His research interests include control technologies for alternating and direct current power systems, power electronic and FACTS, smart measurement and control technologies, and distribution network automation.